HHS Public Access

Author manuscript

Obesity (Silver Spring). Author manuscript; available in PMC 2018 February 25.

Published in final edited form as:

Obesity (Silver Spring). 2017 October ; 25(10): 1745–1753. doi:10.1002/oby.21958.

Incorporating Refractory Period in Mechanical Stimulation Mitigates Obesity-Induced Adipose Tissue Dysfunction in Adult Mice

Vihitaben S. Patel[1], **M. Ete Chan**[1], **Gabriel M. Pagnotti**[1], **Danielle M. Frechette**[1], **Janet Rubin**[2], and **Clinton T. Rubin**[1]

[1]Department of Biomedical Engineering, Stony Brook University, Stony Brook, NY, USA

[2]Department of Medicine, University of North Carolina, Chapel Hill, NC, USA

Abstract

Objective—To determine whether inclusion of a refractory period between bouts of low magnitude mechanical stimulation (LMMS) can curb obesity-induced adipose tissue dysfunction and sequelae in adult mice.

Methods—A diet-induced obesity model with 45kcal% fat diet was employed with intention-to-treat. C57BL/6J mice were weight-matched into four groups: low fat diet (LFD, n=8), high fat diet (HF, n=8), high fat diet with one bout of 30min LMMS (HFv, n=9), and high fat diet with two bouts of 15min LMMS with 5-hour separation (refractory period, RHFv, n=9). 2-week of diet was followed by 6-week of diet+LMMS.

Results—HF and HFv continued gaining body weight and visceral adiposity throughout the experiment, which was mitigated in RHFv. HF and HFv had increased adipocyte hypertrophy, immune cell infiltration (B-cells, T cells, and macrophages) into adipose tissue, adipose tissue inflammation (TNF-α gene expression), and decreased proportion of mesenchymal stem cells in adipose tissue, as compared to LFD, all of which was rescued in RHFv. Glucose intolerance, sequelae of adipose tissue dysfunction, were elevated in HF and HFv, but not in RHFv, as compared to LFD.

Conclusion—Incorporating a 5-hour refractory period between bouts of LMMS attenuates obesity-induced adipose tissue dysfunction and mitigates glucose intolerance.

Keywords

low intensity vibration; adipocyte hypertrophy; chronic inflammation; immunosuppression

Contact Info: Clinton T. Rubin, Ph.D., Department of Biomedical Engineering, Stony Brook University, Stony Brook, NY 11794-2580, Phone: (631) 632-1188, Fax: (631) 632-8577, clinton.rubin@stonybrook.edu.

Disclosure: C.T.R. has authored patents related to the mechanical regulation of metabolic diseases, and is a founder of *Marodyne Medical*. Other authors have nothing to disclose.

Introduction

Obesity continues to grow at an alarming rate in the United States, doubling in the past 30 years, with more than one third of the adult population suffering from this condition [1]. This is a major health concern since obesity increases susceptibility to a range of life-threatening sequelae, such as cardiovascular diseases, hypertension, cancer and type II diabetes (T2D). These obesity-associated comorbidities not only reduce quality of life, but also pose a significant economic burden, costing approximately $147 billion/year in the United States [2]. Thus, it is crucial to develop a cost-effective and widely accessible treatment to obesity.

One of the primary sites affected by obesity is adipose tissue, a metabolically active tissue that functions as a storage compartment for excess energy [3]. Over-consumption during obesity leads to excessive lipid storage in adipocytes, resulting in adipocyte hypertrophy, which can induce fat necrosis and release of pro-inflammatory cytokines [4]. Adipose tissue dysfunction and the chronic inflammatory state associated with obesity have been shown to contribute to insulin resistance and glucose intolerance, the underlying causes for T2D [5]. There is accumulating evidence that exercise, a primary treatment modality for obesity, plays a role in strengthening the immune system and reducing adipose tissue inflammation [6, 7]. While exercise avoids the inherent risks of pharmaceuticals, the demands of daily physical exertion are not easily achieved by the morbidly obese [8].

In contrast to the strenuous exercise, low magnitude mechanical stimulation (LMMS) delivered via low intensity vibration (LIV) has been shown to suppress adipogenesis and adiposity, not by increasing metabolism of existing tissue, but by biasing lineage selection in the mesenchymal stem cell (MSC) differentiation [9-11]. In addition to playing a principal role in adipogenesis, MSC have been shown to exhibit an immunosuppressive effect by regulating proliferation of lymphocytes both *in-vitro* and *in-vivo* and by triggering macrophages to produce anti-inflammatory cytokines, such as IL-10 [12, 13]. Interestingly, LIV has also been shown to play a role in altering immune responses by increasing the bone marrow B-cell population that is depleted by diet-induced obesity [14]. Thus, targeting MSC and the immune system simultaneously via LIV could potentially mitigate the pernicious consequences of obesity. The challenge of using LMMS in adults to treat the obese state is that the sensitivity to mechanical stimulation may have already disappeared [15]. Published work on LMMS shows that the younger the subject - mouse or human - the more effective the signal [16], reflecting an age-dependent decline in cell mechanosensitivity [17].

One potential solution to address reduced mechanosensitivity in adults could be inclusion of a refractory period between loading bouts [18]. At the cellular level, inclusion of a 3-hour refractory period between LMMS bouts has been shown to enhance adipogenesis suppression [20, 21]. In a murine model, incorporation of a 5-hour refractory period between LMMS bouts led to increased MSC population in the bone marrow [22]. Hence, in this experiment we aimed to determine if this effect could be extended at the metabolic level *in-vivo*. We hypothesize that inclusion of a 5-hour refractory-period between bouts of LIV can mitigate obesity-induced adipose tissue dysfunction, and subsequently T2D, in adult mice.

Methods

Diet-Induced Obesity Model and Mechanical Stimulation

All animal protocols were reviewed and approved by Stony Brook University Institutional Animal Care and Use Committee. Starting from 17-week-old, 34 male C57BL/6J mice (*The Jackson Laboratory*, ME) were weight-matched into four groups: low fat diet (LFD, n=8), high fat diet (HF, n=8), high fat diet with one 30-minute bout (1×30) of mechanical stimulation (HFv, n=9), and high fat diet with two 15-minute bouts (2×15) of mechanical stimulation with a 5-hour refractory period between bouts (RHFv, n=9). All mice were single-housed and had *ad libitum* access to food and water. Intention-to-treat model consisted of 2 phases (Figure 1). During both phases, LFD mice were fed 10% kcal from fat diet (58Y2 Van Heek series; *Test Diet*, MO), while HF, HFv and RHFv mice were fed 45% kcal from fat diet (58V8 Van Heek series; *Test Diet*, MO). Phase I (2 weeks) consisted of diet-only treatment to induce obese phenotype. During phase II (6 weeks following phase I), HFv and RHFv mice were mechanically stimulated via LIV protocol [0.2g peak acceleration (1.0g = 9.81 m/s^2), 90 Hz, 5 days/week] for 1×30 and 2×15, respectively, using a vertically oscillating platform (*Marodyne LiV*, FL). During each LIV delivery, the groups that were not being stimulated were sham handled by placing them on an inactive vibration platform. Body weight and calorie intake were measured weekly. At the end of experiment, animals were euthanized via CO^2 inhalation followed by cervical dislocation. Gonadal fat pad weight for each animal was measured at euthanasia.

Quantification of Abdominal Adiposity by Micro-computed Tomography (microCT)

Abdominal adiposity was quantified *in-vivo* using microCT (vivaCT 40; *Scanco Medical Inc.*, PA). Mice were scanned at two time points: at the end of phase I, and at the end of phase II. All scans were performed at 45 kVp, 133 μA, 125 projections per 180°, and 76 μm resolution [23]. During scans, mice were maintained under anesthesia (2% isoflurane inhalation) and placed in a custom-designed foam holder to prevent body movements. Total adipose tissue (TAT) was measured across the abdominal region between L1 and L5 lumbar vertebrae. TAT was further segregated into subcutaneous adipose tissue (SAT) and visceral adipose tissue (VAT) using an automated script [24].

Adipocyte Area Measurement

Half of left gonadal fat pad for each mouse was embedded in paraffin, sectioned (10 μm) and stained with standard hematoxylin and eosin. Three non-consecutive sections from each animal were imaged at three randomly selected areas (total 9 areas per animal) at 400× and were evaluated using ImageJ (*National Institutes of Health*, MD) [25]. The boundary of each adipocyte was manually traced using the ‘Freehand selections’ tool and the area of each adipocyte was measured using the ‘Measure’ tool. All imaging evaluations were performed blind to the experimental group.

Flow Cytometry Analysis

Right gonadal fat pads were dissociated by immersing in collagenase type II (*Worthington Biochemical Corp*, NJ) and by manually straining through a 70μm strainer. Red blood cells

were lysed using 1× Pharmlyse (*BD Biosciences*, CA). A single-cell suspension containing 2×10^6 cells was prepared from each animal to identify MSC [Sca-1(PE)$^+$ CD90.2(APC)$^+$ C-kit(PerCP/Cy5.5)$^+$ CD105(PE/Cy7)$^+$ CD44(Pacific Blue)$^+$], B-cells [B220(PerCP/Cy5.5)$^+$], T cells [CD4(PE)$^+$], and macrophages [F4/80(FITC)$^+$] via flow cytometry (FACSAria, FACSCalibur; *BD Biosciences*, CA) [9, 26-29]. Distinct spectra of emission wavelengths were chosen for each fluorochrome conjugate to avoid overlaps in cell populations.

RNA Extraction and Real-time RT-PCR

Half of left gonadal fat pad from each mouse was preserved in RNAlater (*Life Technologies*, NY). Total RNA was extracted using RNeasy lipid tissue mini kit (*Qiagen*, MD). The amount of RNA was measured using NanoDrop spectrophotometer (*NanoDrop Technologies*, DE). Each RNA sample was diluted to 10 ng/μl. The diluted RNA samples were converted to cDNA using high-capacity cDNA reverse transcription kit (*Life Technologies*, NY). Real time RT-PCR was performed using TaqMan gene expression assays (*Life Technologies*, NY) for tumor necrosis factor alpha (TNF-α, Mm00443258_m1) and insulin receptor substrate 1 (IRS1, Mm01278327_m1). All expression levels were measured with respect to LFD and were normalized to Rn18s (Mm03928990_g1, *Life Technologies*, NY) [30].

Plasma Insulin Measurement and Glucose Tolerance Test (GTT)

Plasma insulin measurement and GTT were performed at the end of phase II. After overnight fasting, blood was collected via tail tip transection and plasma was isolated by centrifugation. Fasting plasma insulin was measured using a mouse insulin ELISA kit with rat insulin as a standard (*EMD Millipore*, MO). Fasting blood glucose was measured using ACCU-CHEK Aviva system (*Roche Diagnostics*, Switzerland). Mice were then injected intraperitoneally with 20% dextrose solution in sterile saline (*Sigma-Aldrich*, MO) at the dosage of 0.75 g dextrose per 1 kg of body weight. Blood glucose was measured at 15, 30, 45, 60, 90, and 120 minutes after the injection. Glucose intolerance was measured by calculating the area under the curve in blood glucose vs. time graph using trapezoidal method.

Statistical Analysis

Normality was accessed via Shapiro-Wilk test with $\alpha=0.05$. Normally distributed datasets were analyzed using one-way ANOVA (Tukey's post-hoc test) and presented as mean±SD, whereas non-normally distributed datasets were analyzed using Kruskal-Wallis test (Dunn's post-hoc test) (*Graphpad Prism*, CA) and presented as box plot (median, interquartile range, minimum and maximum). Correlations were determined by calculating the Pearson correlation coefficient. P-value of $p<0.05$ was considered significant. Outliers were determined via Grubbs' test with $\alpha=0.01$. One of the RHFv animal's data was excluded from all data analyses due to the animal's sickness towards the end of the experiment.

Results

Increased Calorie Intake with High Fat Diet

All high fat diet groups had higher calorie intake compared to LFD throughout the experiment. The largest difference in calorie intake was seen during the first week, where HF, HFv and RHFv had 61%, 58% and 52% higher calorie intake, respectively, as compared to LFD ($p<0.05$, Figure 2A).

Increased Body Weight and Gonadal Fat Weight with High Fat Diet

All animals on high fat diet were 15% heavier as compared to LFD at the end of phase I ($p<0.05$, Figure 2B). During phase II, while LFD maintained their body weight, HF and HFv body weight increased by 11% and 9%, respectively ($p<0.05$ compared to LFD). RHFv showed slowed progression in weight gain with only a 5% increase in body weight during phase II (p=ns compared to LFD, Figure 2C). Gonadal fat pad weight increased in HF (2028±528 mg), HFv (1893±368 mg), and RHFv (1648±507 mg), as compared to LFD (549±99 mg) ($p<0.05$, Figure 2D).

Effect of High Fat Diet and LIV on Abdominal Adiposity

At the end of phase I, high fat diet led to increased TAT, SAT and VAT in HF, HFv and RHFv, as compared to LFD ($p<0.05$, Figure 3B). During phase II, HF, HFv and RHFv showed continued increase in TAT (55%, 41%, 43%, respectively, $p<0.05$, Figure 3C). While SAT increased by 29% and 54%, VAT increased by 43% and 37% in HFv and RHFv, respectively, after 6 weeks of LIV intervention. HF and HFv showed significant increase in VAT (5462% and 3988%, respectively) during phase II, as compared to LFD ($p<0.05$). Although not significantly different from HF or HFv, RHFv showed mitigated increase in VAT (3458% compared to LFD, p=ns) during phase II, demonstrating prevention in VAT gain with 2×15 LIV.

Adipocyte Hypertrophy in Obesity Mitigated by 2×15 LIV

Representative sections of adipocytes from gonadal adipose tissue are shown in Figure 4A. While median adipocyte area of LFD was 1926 μm^2, median adipocyte areas in HF and HFv increased to 2944 μm^2 and 3177 μm^2, respectively ($p<0.05$, Figure 4B). Although still significantly higher than LFD, median adipocyte area of RHFv (2478 μm^2) reduced by 15% ($p<0.05$) and 22% ($p<0.05$) as compared to HF and HFv, respectively.

Obesity Increases Immune Cell Infiltration and Inflammation in Adipose Tissue

While B-cell population in HF and HFv increased by 203% and 240%, respectively ($p<0.05$), increase was limited to 155% in RHFv (p=ns), as compared to LFD (Figure 5A). Similarly, $CD4^+$ T cell population in HF, HFv, and RHFv increased by 150% ($p<0.05$), 132% ($p<0.05$), and 94% (p=ns), respectively, as compared to LFD (Figure 5B). Following the same trend, macrophage population in HF, HFv, and RHFv increased by 137% ($p<0.05$), 152% ($p<0.05$), and 108% (p=ns), respectively, as compared to LFD (n=7 for LFD, one data-point excluded as outlier) (Figure 5C). TNF-α gene expression in gonadal adipose tissue increased in HF (n=7 in HF, one data-point excluded as outlier) and HFv by 108%

(p<0.05) and 67% (p<0.05), respectively, while by 53% (p=ns) in RHFv as compared to LFD (Figure 5D).

Depleted Percentage of MSC (MSC%) in Adipose Tissue during Obesity Partially Restored with 2×15 LIV

MSC in gonadal adipose tissue were quantified via flow cytometric analysis as shown in Figure 6A. MSC% compared to live cells in adipose tissue was lower in HF, HFv and RHFv by 55%, 43% and 33%, respectively, as compared to LFD (p<0.05). MSC% in RHFv (50%, p<0.05), but not in HFv (28%, p=ns), was significantly elevated as compared to HF (Figure 6B). In addition, MSC% exhibited a negative correlation with adipose tissue expression of TNF-α (r=-0.48, p<0.05) (Figure 6C).

Obesity-Induced Glucose Intolerance Mitigated by 2×15 LIV

Fasting blood glucose was similar in all groups. Although not significantly different, the peak blood glucose, observed at 15min after intraperitoneal injection of dextrose, was elevated in HF, HFv, and RHFv, as compared to LFD (Figure 7A). While HF and HFv blood glucose levels remained elevated until 90min after glucose injection as compared to LFD, RHFv had returned to baseline by this time. Glucose intolerance elevated by 15% in both HF and HFv (p<0.05), while the increase was limited to 5% in RHFv (p=ns), as compared to LFD (Figure 7B).

Insulin Resistance during Obesity Improved by 2×15 LIV

As shown in Figure 7C, while high fat diet feeding resulted in hyperinsulinemia in HF and HFv as compared to LFD (238% and 189% higher fasting plasma insulin, respectively, p<0.05), RHFv attenuated hyperinsulinemia (126% higher fasting plasma insulin as compared to LFD, p=ns). Adipose tissue gene expression of IRS1, a key player in insulin signaling, reduced by 30% in HF as compared to LFD (p<0.05). IRS1 expression significantly increased in RHFv (31%, p<0.05), but not in HFv (2%, p=ns), as compared to HF (Figure 7D).

Discussion

Current treatments for obesity and related comorbidities in the form of lifestyle, pharmacological and/or surgical interventions demonstrate limited success due to poor compliance, ineffectiveness, complications, morbidity, and/or mortality [31, 32]. In this study, we investigate the ability of LMMS, as an alternative to exercise, to suppress obesity-induced adipose tissue dysfunction and its sequelae, such as impaired glucose metabolism, in mice. Adult mice were chosen to better represent the pathogenesis observed in majority of patients diagnosed with obesity [1]. Here, we demonstrate that 2×15 LIV, but not 1×30 LIV, successfully mitigates obesity-induced adipose tissue dysfunction and its sequelae in adult mice.

There are a few limitations associated with this study. Control mice were switched from normal chow (13% kcal from fat) to low fat diet (10% kcal from fat) before beginning the study, which might have limited their adiposity gain more than if they were treated as age-

matched control. However, LFD and HFD used here enabled us to keep calories consumed from protein consistent between groups, giving a better comparison for effects of fat consumption. In addition, we have evaluated gonadal adipose tissue, as a representative for visceral adipose depot, throughout the study and we do acknowledge that there might be site-specific physiological and functional differences in other visceral and subcutaneous adipose depots, and future studies can be done to evaluate these differences. Data interpretation for the impact of 2×15 LIV was limited to not having a significant difference between LFD and RHFv, rather than a significant difference between HF and RHFv (with exception of adipocyte hypertrophy, MSC% in adipose tissue, and IRS1 expression in adipose tissue).

Evaluating gross changes in body habitus, 2 weeks of high fat diet induced the obese phenotype, as quantified by increased body weight and abdominal adiposity, before starting the LMMS treatment. All mice on high fat diet, including those subjected to LMMS, continued to gain body weight and abdominal adiposity throughout the experiment, reaffirming previous studies [9, 10, 14]. Progression in weight gain was slowed by incorporating a refractory period between loading bouts (RHFv), limiting the weight-gain to 5% over the 6 weeks of phase II, as compared to the 11% in HF and 9% in HFv, acquired over the same period. Interestingly, despite the continued increase in total adipose tissue measured in RHFv, the distribution of abdominal adipose tissue shifted as compared to HF and HFv, with the gain in RHFv a result of increase in subcutaneous adipose tissue (SAT), while the gain in HF and HFv a result of an increase in visceral adipose tissue (VAT). Under normal physiological condition, SAT is capable of creating new adipocytes to store excess energy intake, a function that gets impaired during obesity [33]. We hypothesize that 2×15 LIV promotes adipogenesis in SAT, increasing its storage capability, to avoid fat accumulation in viscera. Increased visceral adiposity has been associated with increased likelihood of cardiovascular diseases, impaired glucose metabolism, development of insulin resistance, and has overall been shown to be a better predictor of mortality than subcutaneous adiposity [34]. Hence, fat redistribution with 2×15 LIV, toward SAT and away from VAT, suggests a shift to a healthier body habitus.

Following changes in adipose tissue distribution, obesity also led to adipocyte hypertrophy in gonadal fat tissue, paralleled with increased infiltration of B-cells, $CD4^+$ T cells, and macrophages within the tissue, as quantified by flow cytometry. While B-cells and $CD4^+$ T cells play a role in adaptive immunity [35], macrophages are known to secrete TNF-α, a proinflammatory cytokine [36]. Here we show elevated gene expression for TNF-α in the adipose tissue from obese mice as compared to LFD. 2×15, but not 1×30, LIV resulted in significant suppression of adipocyte hypertrophy, and a concomitant reduction in immune cell infiltration in adipose tissue, leading to reduced expression of TNF-α in adipose tissue. Since MSC have been shown to play a role in immunomodulation and immunosuppression [12, 13], we further quantified the MSC population in gonadal adipose tissue. While adipose tissue MSC population decreased with obesity, it was significantly restored with 2×15 LIV. It is still unclear as to what causes the increase in adipose tissue MSC with 2×15 LIV. Some of the possible reasons could be increased proliferation of existing adipose tissue MSC, decreased differentiation of adipose tissue MSC into adipocytes, or increased migration of bone marrow MSC into adipose tissue [10, 20, 37]. We also observed a significant negative

correlation between MSC and inflammation in adipose tissue, indicating an association between the variables such that as MSC in adipose tissue increases, inflammation in the tissue decreases. Although the relationship is not causative as shown, MSC's role in immunosuppression needs to be more accurately determined to serve as a unique strategy for combating obesity-associated adipose tissue dysfunction.

As sequelae of adipose tissue dysfunction, high fat diet resulted in impaired glucose metabolism. HF had significantly higher glucose intolerance, as compared to LFD, which was successfully mitigated by 2×15 LIV, but not by 1×30 LIV. Interestingly, the impaired glucose tolerance in HF and HFv was a result of insulin resistance, as evident by hyperinsulinemia and reduced expression of IRS1 in gonadal fat. IRS1 is an important player in the insulin-signaling pathway, which can drive inactivation of PI3K, leading to hyperglycemia, hyperinsulinemia and insulin resistance [38]. Alternatively, RHFv showed mitigated hyperinsulinemia and increased expression of IRS1 in gonadal fat as compared to HF, indicating reduced insulin resistance. The effectiveness of 2×15 LIV, but not of 1×30 LIV, in improving glucose metabolism is in contrast to the previous study where one bout of 20-minute vibration/day shows improved glucose metabolism [39]. However, this previous study utilized young mice, reaffirming that the mechanosensitivity might indeed be age-dependent and that the inclusion of a refractory period in LMMS can boost the declined mechanosensitivity.

The beneficial effect of 2×15, but not 1×30 LIV, in rescuing obesity-induced adipose tissue dysfunction and impaired glucose metabolism in adults suggests that the scheduling of LMMS is of more importance than the total duration. This result reinforces the outcomes from previous studies that demonstrate an enhanced response towards mechanical stimulation or exercise regime with incorporation of a refractory period between bouts or incorporation of a rest period between individual loading cycles [18, 20, 40]. Previous *in-vitro* study demonstrates that MSC respond to LMMS through coupling of cytoskeleton and nucleus and that the first bout of LMMS leads to perinuclear cytoskeletal remodeling in the form of increased focal adhesions and increased RhoA activity, which leads to amplified mechanical response to the second bout of LMMS [19]. Salutary effects of 2×15 LIV can then be partially attributed to cytoskeletal reorganization of mechanosensitive cells, such as MSC, *in-vivo*.

Conclusion

Overall, this study demonstrates the body habitus changes consistent with obesity, such as increased adiposity within the visceral cavity as well as increased adipocyte size. The consequently elevated adipose tissue inflammation may contribute to increased insulin resistance and glucose intolerance. While a single bout of LMMS was not successful in reducing adipose tissue dysfunction and sequelae caused by chronic obesity, incorporating a 5-hour refractory period between two bouts of LMMS reduced visceral adiposity, adipocyte size, adipose tissue inflammation and increased MSC population in the adipose tissue, resulting in improved insulin sensitivity and glucose metabolism. These data may provide insight into the means by which exercise provides salutary signals to those struggling with obesity, and imports that the *scheduling* of the physical activity may be as critical as the

activity itself. And while LIV can only be viewed as a surrogate for exercise, it does provide a means of delivering a signal that mitigates some of the complications of obesity while not requiring strenuous exertion.

Acknowledgments

Authors are grateful for the technical assistance provided by Alyssa Tuthill, Divya Krishnamoorthy, Tee Pamon, Jeyantt Sankaran, Shabab Hussain, and Ariel Yang.

Funding: This work was supported by National Institute of Health through National Institute of Arthritis and Musculoskeletal and Skin Diseases grant AR-43498 and National Institute of Biomedical Imaging and Bioengineering grant EB-14351.

References

1. Ogden CL, Carroll MD, Kit BK, Flegal KM. Prevalence of childhood and adult obesity in the united states, 2011-2012. Jama. 2014; 311:806–814. [PubMed: 24570244]
2. Finkelstein EA, Trogdon JG, Cohen JW, Dietz W. Annual medical spending attributable to obesity: Payer-and service-specific estimates. Health Aff (Millwood). 2009; 28:w822–831. [PubMed: 19635784]
3. Fantuzzi G. Adipose tissue, adipokines, and inflammation. J Allergy Clin Immunol. 2005; 115:911–919. quiz 920. [PubMed: 15867843]
4. Ghigliotti G, Barisione C, Garibaldi S, et al. Adipose tissue immune response: Novel triggers and consequences for chronic inflammatory conditions. Inflammation. 2014; 37:1337–1353. [PubMed: 24823865]
5. Qatanani M, Lazar MA. Mechanisms of obesity-associated insulin resistance: Many choices on the menu. Genes Dev. 2007; 21:1443–1455. [PubMed: 17575046]
6. Vieira VJ, Valentine RJ, Wilund KR, Antao N, Baynard T, Woods JA. Effects of exercise and low-fat diet on adipose tissue inflammation and metabolic complications in obese mice. Am J Physiol Endocrinol Metab. 2009; 296:E1164–1171. [PubMed: 19276393]
7. Kawanishi N, Mizokami T, Yano H, Suzuki K. Exercise attenuates m1 macrophages and cd8+ t cells in the adipose tissue of obese mice. Med Sci Sports Exerc. 2013; 45:1684–1693. [PubMed: 23954991]
8. Villareal DT, Chode S, Parimi N, et al. Weight loss, exercise, or both and physical function in obese older adults. N Engl J Med. 2011; 364:1218–1229. [PubMed: 21449785]
9. Luu YK, Capilla E, Rosen CJ, et al. Mechanical stimulation of mesenchymal stem cell proliferation and differentiation promotes osteogenesis while preventing dietary-induced obesity. J Bone Miner Res. 2009; 24:50–61. [PubMed: 18715135]
10. Luu YK, Pessin JE, Judex S, Rubin J, Rubin CT. Mechanical signals as a non-invasive means to influence mesenchymal stem cell fate, promoting bone and suppressing the fat phenotype. Bonekey Osteovision. 2009; 6:132–149. [PubMed: 22241295]
11. Rubin CT, Capilla E, Luu YK, et al. Adipogenesis is inhibited by brief, daily exposure to high-frequency, extremely low-magnitude mechanical signals. Proc Natl Acad Sci U S A. 2007; 104:17879–17884. [PubMed: 17959771]
12. Bartholomew A, Sturgeon C, Siatskas M, et al. Mesenchymal stem cells suppress lymphocyte proliferation in vitro and prolong skin graft survival in vivo. Exp Hematol. 2002; 30:42–48. [PubMed: 11823036]
13. Nemeth K, Leelahavanichkul A, Yuen PS, et al. Bone marrow stromal cells attenuate sepsis via prostaglandin e(2)-dependent reprogramming of host macrophages to increase their interleukin-10 production. Nat Med. 2009; 15:42–49. [PubMed: 19098906]
14. Chan ME, Adler BJ, Green DE, Rubin CT. Bone structure and b-cell populations, crippled by obesity, are partially rescued by brief daily exposure to low-magnitude mechanical signals. Faseb j. 2012; 26:4855–4863. [PubMed: 22898923]

15. Klein-Nulend J, Sterck JG, Semeins CM, et al. Donor age and mechanosensitivity of human bone cells. Osteoporos Int. 2002; 13:137–146. [PubMed: 11908490]
16. Gilsanz V, Wren TA, Sanchez M, Dorey F, Judex S, Rubin C. Low-level, high-frequency mechanical signals enhance musculoskeletal development of young women with low bmd. J Bone Miner Res. 2006; 21:1464–1474. [PubMed: 16939405]
17. Uzer G, Fuchs RK, Rubin J, Thompson WR. Concise review: Plasma and nuclear membranes convey mechanical information to regulate mesenchymal stem cell lineage. Stem Cells. 2016; 34:1455–1463. [PubMed: 26891206]
18. Robling AG, Burr DB, Turner CH. Recovery periods restore mechanosensitivity to dynamically loaded bone. J Exp Biol. 2001; 204:3389–3399. [PubMed: 11606612]
19. Uzer G, Thompson WR, Sen B, et al. Cell mechanosensitivity to extremely low-magnitude signals is enabled by a linced nucleus. Stem Cells. 2015; 33:2063–2076. [PubMed: 25787126]
20. Sen B, Xie Z, Case N, Styner M, Rubin CT, Rubin J. Mechanical signal influence on mesenchymal stem cell fate is enhanced by incorporation of refractory periods into the loading regimen. J Biomech. 2011; 44:593–599. [PubMed: 21130997]
21. Sen B, Guilluy C, Xie Z, et al. Mechanically induced focal adhesion assembly amplifies anti-adipogenic pathways in mesenchymal stem cells. Stem Cells. 2011; 29:1829–1836. [PubMed: 21898699]
22. Appiah-Nkansah K. Integration of refractory periods in the administration of low-magnitude mechanical signals increases mesenchymal stem cell numbers in the bone marrow. Stony Brook University. 2011:25–27. Master of Science.
23. Judex S, Luu YK, Ozcivici E, Adler B, Lublinsky S, Rubin CT. Quantification of adiposity in small rodents using micro-ct. Methods. 2010; 50:14–19. [PubMed: 19523519]
24. Luu YK, Lublinsky S, Ozcivici E, et al. In vivo quantification of subcutaneous and visceral adiposity by micro-computed tomography in a small animal model. Med Eng Phys. 2009; 31:34–41. [PubMed: 18486521]
25. Luu YK, Ozcivici E, Capilla E, et al. Development of diet-induced fatty liver disease in the aging mouse is suppressed by brief daily exposure to low-magnitude mechanical signals. Int J Obes (Lond). 2010; 34:401–405. [PubMed: 19935747]
26. Blazquez-Martinez A, Chiesa M, Arnalich F, Fernandez-Delgado J, Nistal M, De Miguel MP. C-kit identifies a subpopulation of mesenchymal stem cells in adipose tissue with higher telomerase expression and differentiation potential. Differentiation. 2014; 87:147–160. [PubMed: 24713343]
27. Ying W, Tseng A, Chang RC, et al. Mir-150 regulates obesity-associated insulin resistance by controlling b cell functions. Sci Rep. 2016; 6:20176. [PubMed: 26833392]
28. Deng T, Lyon CJ, Minze LJ, et al. Class ii major histocompatibility complex plays an essential role in obesity-induced adipose inflammation. Cell Metab. 2013; 17:411–422. [PubMed: 23473035]
29. Weisberg SP, McCann D, Desai M, Rosenbaum M, Leibel RL, Ferrante AW Jr. Obesity is associated with macrophage accumulation in adipose tissue. J Clin Invest. 2003; 112:1796–1808. [PubMed: 14679176]
30. Zhang J, Tang H, Zhang Y, et al. Identification of suitable reference genes for quantitative rt-pcr during 3t3-l1 adipocyte differentiation. Int J Mol Med. 2014; 33:1209–1218. [PubMed: 24626784]
31. Foreyt JP, Poston WS 2nd. The challenge of diet, exercise and lifestyle modification in the management of the obese diabetic patient. Int J Obes Relat Metab Disord. 1999; 23(Suppl 7):S5–11. [PubMed: 10455465]
32. Peckmezian T, Hay P. A systematic review and narrative synthesis of interventions for uncomplicated obesity: Weight loss, well-being and impact on eating disorders. J Eat Disord. 2017; 5:15. [PubMed: 28469914]
33. Gustafson B, Hammarstedt A, Hedjazifar S, Smith U. Restricted adipogenesis in hypertrophic obesity: The role of wisp2, wnt, and bmp4. Diabetes. 2013; 62:2997–3004. [PubMed: 23970518]
34. Ritchie SA, Connell JM. The link between abdominal obesity, metabolic syndrome and cardiovascular disease. Nutr Metab Cardiovasc Dis. 2007; 17:319–326. [PubMed: 17110092]
35. Travers RL, Motta AC, Betts JA, Bouloumie A, Thompson D. The impact of adiposity on adipose tissueresident lymphocyte activation in humans. Int J Obes (Lond). 2015; 39:762–769. [PubMed: 25388403]

36. Unoki H, Bujo H, Jiang M, Kawamura T, Murakami K, Saito Y. Macrophages regulate tumor necrosis factor-alpha expression in adipocytes through the secretion of matrix metalloproteinase-3. Int J Obes (Lond). 2008; 32:902–911. [PubMed: 18283281]

37. Uzer G, Pongkitwitoon S, Chan ME, Judex S. Vibration induced osteogenic commitment of mesenchymal stem cells is enhanced by cytoskeletal remodeling but not fluid shear. J Biomech. 2013; 46:2296–2302. [PubMed: 23870506]

38. Guo S. Insulin signaling, resistance, and the metabolic syndrome: Insights from mouse models into disease mechanisms. J Endocrinol. 2014; 220:T1–t23. [PubMed: 24281010]

39. McGee-Lawrence ME, Wenger KH, Misra S, et al. Whole-body vibration mimics the metabolic effects of exercise in male leptin receptor deficient mice. Endocrinology. 2017

40. Srinivasan S, Weimer DA, Agans SC, Bain SD, Gross TS. Low-magnitude mechanical loading becomes osteogenic when rest is inserted between each load cycle. J Bone Miner Res. 2002; 17:1613–1620. [PubMed: 12211431]

Study Importance Questions

1. What is already known about this subject?

- Adipose tissue functions as more than just a passive lipid storage, also playing an important role in synthesizing various hormones and growth factors and releasing triglycerides, cytokines and adipokines. Importantly, fat depots are one of the first sites to be altered by obesity.
- Obesity-induced adipose tissue dysfunction and a chronic inflammatory state can lead to defects in glucose metabolism.
- Mechanical stimulation via low intensity vibration has been shown to suppress adipogenesis and alter immune system by increasing bone marrow B-cell population depleted by obesity.

2. What does your study add?

- In addition to gross changes in adipose tissue, obesity also depletes the mesenchymal stem cell (MSC) pool in the gonadal adipose tissue. MSC are shown here to have a negative correlation with adipose tissue inflammation.
- Mechanical stimulation, as a surrogate to exercise, can be utilized to curb obesity-induced adipose tissue dysfunction and impaired glucose metabolism.
- Adding a refractory period between bouts of mechanical stimulation is more beneficial in curbing obesity-induced adversities in adults. Hence, it is not only the total duration, but also the scheduling of mechanical stimulation that is critically important.

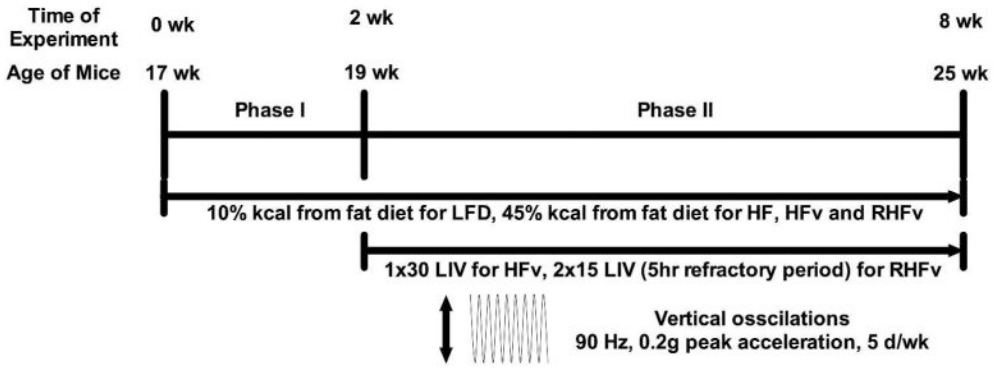

Figure 1.

Experimental timeline consisting of 2 phases. During Phase I (initial 2 weeks), while LFD mice were fed 10% kcal from fat diet, HF, HFv and RHFv mice were fed 45% kcal from fat diet, to induce the obese phenotype. During phase II (6 weeks following phase I), HFv and RHFv mice underwent LIV stimulation (vertical oscillations, 90Hz, 0.2g peak acceleration, 5 days/week) for one bout of 30 minutes per day (1×30) and two bouts of 15 minutes per day with 5-hour refractory period (2×15), respectively. All mice were euthanized at 8 weeks following the start of experiment at the age of 25wo.

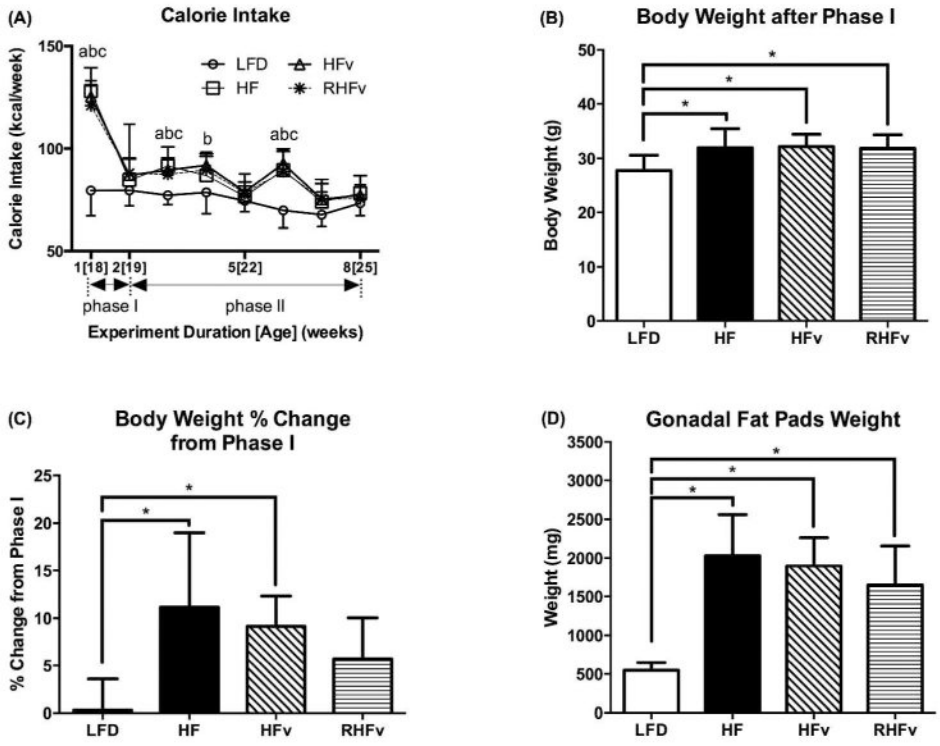

Figure 2.

Diet-induced obesity model. (A) Mice on high fat diet (HF, HFv, and RHFv) had increased calorie intake compared to mice fed a low fat diet throughout the experiment. (B) Increased body weight in HF, HFv and RHFv at the end of phase I (two weeks on high fat diet), as compared to LFD, prior to LIV treatment ($p<0.05$). (C) Percent change in body weight of each animal during phase II, after six weeks of LIV treatment. Continued increase in body weight in HF and HFv ($p<0.05$), slowed progression in RHFv (p=ns), as compared to LFD. (D) Increased gonadal fat pad weight in all high fat diet animals as measured after euthanasia ($p<0.05$). $^{a,b,c}p<0.05$ vs. LFD for HF, HFv and RHFv, respectively. *$p<0.05$. All datasets were normally distributed and data is presented as mean±SD.

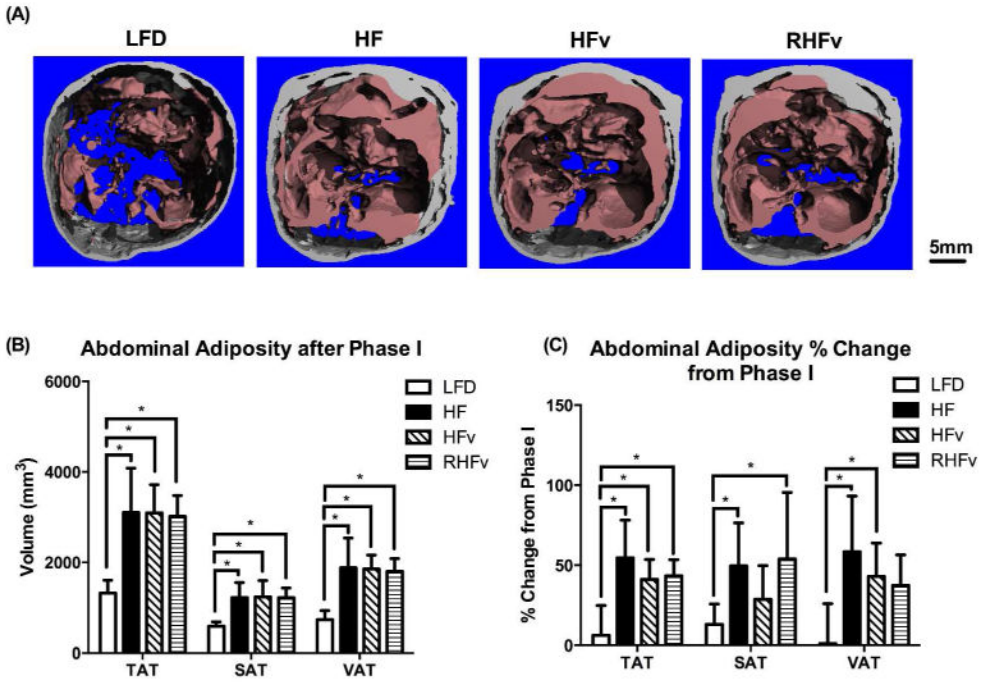

Figure 3.

Abdominal adiposity. (A) Representative microCT sections of transverse abdominal region to demonstrate the distribution of SAT (grey) and VAT (pink) in LFD, HF, HFv and RHFv (from left to right) at the end of phase II. (B) Increased total, subcutaneous, and visceral abdominal adiposity (TAT, SAT, and VAT, respectively) in all high fat diet groups at the end of phase I, as compared to LFD, before LIV treatment ($p<0.05$). (C) Percent change in TAT, SAT and VAT of each animal from the end of phase I. Continued increase in TAT of HF, HFv and RHFv ($p<0.05$). While increase in TAT was a result of increased VAT for HF and HFv, RHFv promoted SAT gain and mitigated VAT gain. *$p<0.05$. All datasets were normally distributed and data is presented as mean±SD.

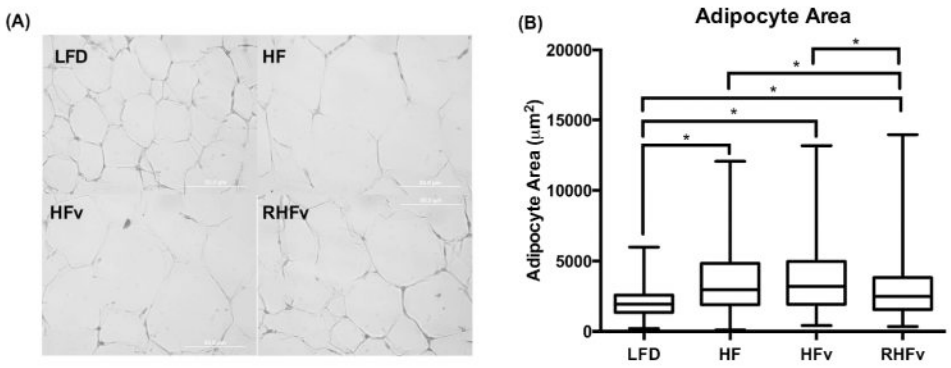

Figure 4.

Adipocyte hypertrophy. (A) Representative histological sections of gonadal fat pads (40× magnification) stained with hematoxylin and eosin to detect adipocyte boundaries. (B) Compared to LFD, increased adipocyte area due to high fat diet in HF, HFv and RHFv. Median adipocyte area significantly decreased in RHFv but not in HFv, compared to HF. *$p<0.05$. Dataset was not normally distributed and is presented as median, interquartile range, minimum and maximum.

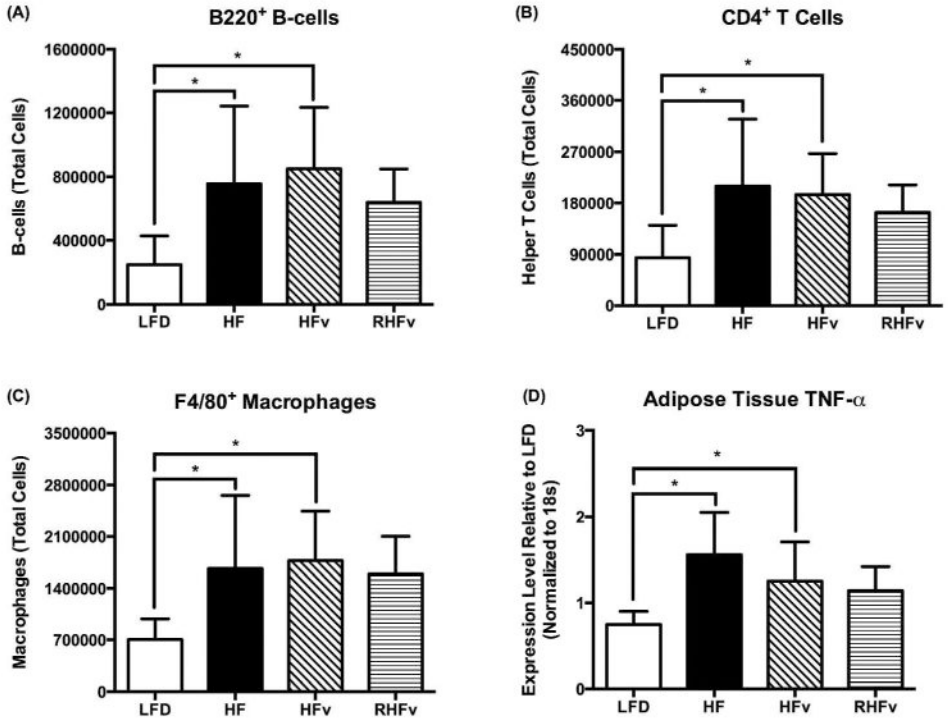

Figure 5.

Adipose tissue inflammation. Significantly increased infiltration of $B220^+$ B-cells (A), $CD4^+$ T cells (B), and $F4/80^+$ macrophages (C) in the gonadal adipose tissue of HF and HFv, but not RHFv, compared to LFD. (D) Significantly increased gene expression of TNF-α, a pro-inflammatory cytokine, in the gonadal adipose tissue of HF and HFv, but not RHFv, compared to LFD. *$p<0.05$. All datasets were normally distributed and data is presented as mean±SD.

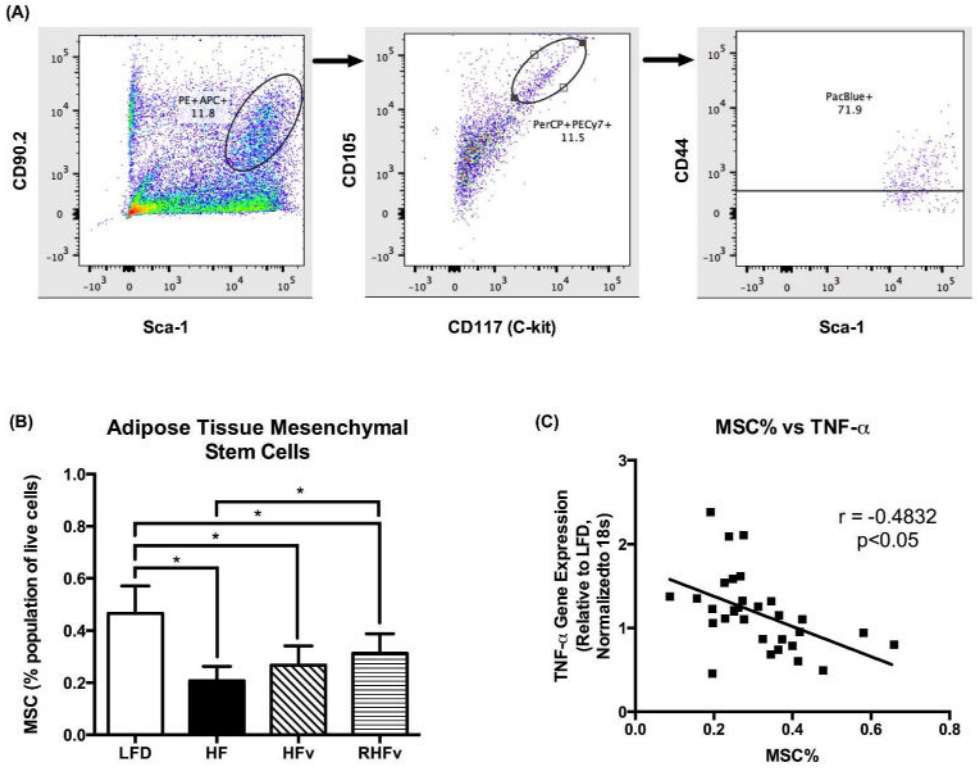

Figure 6.

Adipose tissue mesenchymal stem cells and inflammation. (A) Representative gating scheme to determine mesenchymal stem cell population (Sca-1^{+}CD90.2^{+}CD117^{+}CD105^{+}CD44^{+}) in adipose tissue. (B) Decreased adipose tissue MSC% in HF, HFv and RHFv, compared to LFD. MSC% rescued in RHFv, but not in HFv, compared to HF. (C) Negative correlation between adipose tissue MSC% and adipose tissue TNF-α expression (r=-0.4832, p<0.05). *p<0.05. All datasets were normally distributed and data is presented as mean±SD.

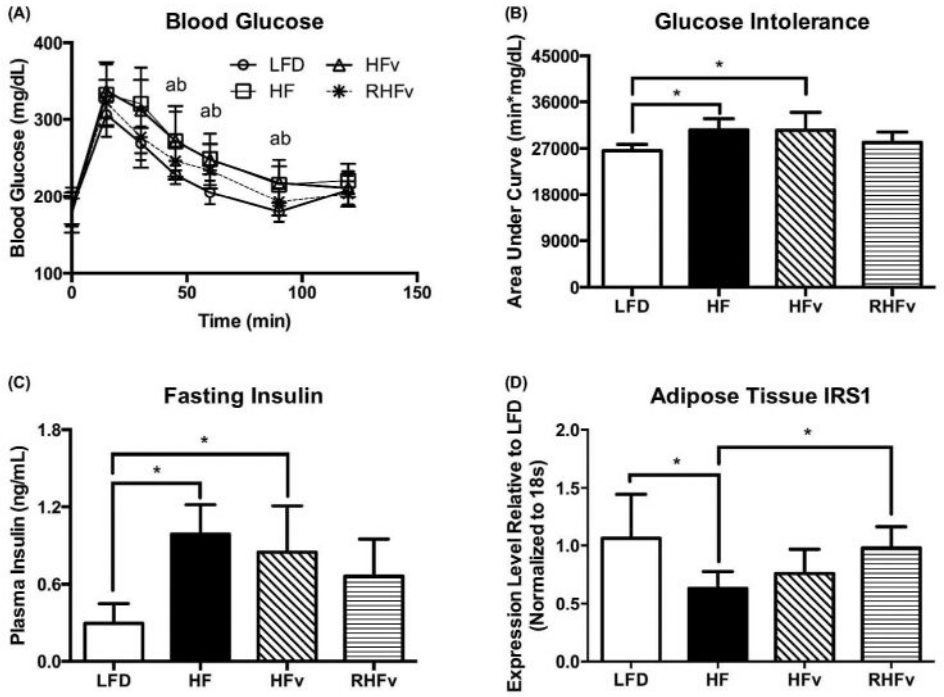

Figure 7.

Glucose intolerance as a sequelae of adipose tissue dysfunction. (A) Change in blood glucose for 2 hours after intraperitoneal dextrose injection. Improved blood glucose elimination in RHFv compared to HF and HFv. (B) Increased glucose intolerance in HF and HFv, but not in RHFv, compared to LFD as measured by the area under the blood glucose curve in Figure 6A. (C) Increased fasting insulin in HF and HFv, but not in RHFv, compared to LFD. (D) Compared to LFD, reduced expression of IRS1, an insulin receptor, in adipose tissue of HF due to high fat diet. Elevated expression of IRS1 in RHFv as compared to HF, despite high fat diet. $^{a,b}p<0.05$ vs. LFD for HF and HFv, respectively. *$p<0.05$. All datasets were normally distributed and data is presented as mean±SD.